

Contributions of the Active and Passive Components of the Cytoskeletal Prestress to Stiffening of Airway Smooth Muscle Cells

NOAH ROSENBLATT,¹ SHAOHUA HU,² BÉLA SUKI,¹ NING WANG,³ and DIMITRIJE STAMENIČIĆ¹

¹Department of Biomedical Engineering, Boston University, 44 Cummington St., Boston, MA 02215, USA; ²Physiology Program, Department of Environmental Health, Harvard School of Public Health, Boston, MA 02115, USA; and ³Department of Mechanical Science and Engineering, University of Illinois at Urbana-Champaign, Urbana, IL 61801, USA

(Received 22 May 2006; accepted 30 October 2006; published online: 6 December 2006)

Abstract—Airway smooth muscle cells exhibit stiffening during contractile activation. This stiffening may be interpreted as a result of the stabilizing influence of the mechanical prestress stored within the cytoskeleton (CSK). However, *in vivo*, airway smooth muscle cells contract while simultaneously experiencing breathing-induced stretching. Excessive stretching of cells could cause actin–myosin crosslinks, and possibly other cytoskeletal filaments, to break, thereby leading to dissipation of the prestress and inhibition of further cell stiffening. The aim of this study is to investigate the stiffening behavior of individual human airway smooth muscle (HASM) cells exposed to a combination of substrate stretching, contractile activation and relaxation. We treated cultured HASM cells with either contractile (histamine) or relaxing (DBcAMP) pharmacological agonists and used magnetic cytometry technique to investigate the stiffening behavior of these cells during uniform substrate stretching (0–30%). Cells that were not treated, as well as those treated with histamine, exhibited increasing stiffening during stretching up to 20% of substrate strain, with additional stiffening becoming inhibited for substrate strains of 20–30%. In contrast, in cells treated with DBcAMP, stretching produced moderate but continuous stiffening with increasing substrate strain. These results indicate that both active and passive components of the prestress contribute to cell stiffening. We also observed that cells permeabilized with saponin exhibited stiffening at low levels (< 10%) of substrate stretching, similar to non-permeabilized cells, but not at high levels (10–30%) of stretching, where stiffening was inhibited. These data suggest that at low levels of substrate strains the relative contributions of ion channel activation as well as actin and focal adhesion remodeling are less important for stiffening than passive distension of the CSK. Taken together, our results suggest that both the active and passive components of the cytoskeletal prestress contribute to the stiffening behavior of HASM cells under physiological conditions, but that at high levels of cellular distensions there is a possible tradeoff between these two components with the contribution from the passive component becoming increasingly more important.

Keywords—Cytoskeleton, Prestress, Contractility, Elastic modulus, Stiffening, Hysteresivity.

INTRODUCTION

During the past decade, a number of studies have shown that mechanical distending stress borne by the cytoskeleton (CSK) stabilizes cell shape.^{1,5,15,22,23,25,29–33} This stress, often referred to as a prestress, is primarily generated by the cytoskeletal contractile machinery and can be altered either actively, by pharmacological contractile and relaxant agonists, or passively, by mechanical distension of the cell. It has been observed that a systematic increase in this prestress is paralleled by a systematic increase in cell stiffness.^{5,15,22,23,25,29,32,33} One explanation for this stiffening behavior is offered by the cellular tensegrity model.¹⁶ According to this model, cytoskeletal prestress confers shape stability to the CSK by constraining its internal degrees of freedom.^{26,27} Consequently, the greater the prestress in the CSK, the greater its resistance to deformation under externally applied loads and therefore the greater its stiffness. An *a priori* prediction that stems from this property is that the stiffness increases in a direct proportion with increasing prestress.^{26,27,33} We have recently experimentally confirmed this relationship in cultured airway smooth muscle cells where the prestress was modulated by different doses of pharmacological contractile and relaxant agonists.^{32,33} Since *in vivo* airway smooth muscle cells adhere to an extracellular matrix that is exposed to breathing-induced stretching, this also causes mechanical distension of the CSK and thereby modulates the cytoskeletal prestress. According to the tensegrity model, one would expect the stiffness to increase continuously with increasing substrate stretching. If, however, stretching the extracellular matrix were to lead to the disruption of actin–myosin contractile crosslinks, or interfere with other,

Address correspondence to Dimitrije Stamenović, Department of Biomedical Engineering, Boston University, 44 Cummington St., Boston, MA 02215, USA. Electronic mail: dimitrij@bu.edu

non-contractile cytoskeletal filaments, this would offset the buildup of prestress and thereby impede cell stiffening. In this study, we investigated the effect of stretching on cell stiffening at different levels of cell contractility. Understanding this relationship is important since stiffness and stiffening are critical for a host of life-sustaining cell functions including adhesion, spreading, orientation, division, and motility.

We used the established magnetic cytometry technique^{5,7} to measure stiffness in cultured airway smooth muscle cells during uniform substrate stretching²³ in the presence of contractile or relaxing pharmacological agonists. Our results showed that cell stiffness increased with increasing cell stretching up to $\sim 20\%$ of substrate strain and that further stretching inhibited further increase in cell stiffening. However, stretching did not appear to inhibit stiffening associated with the passive component of the cytoskeletal prestress, which contributes significantly to cell stiffness at excessive substrate strains.

METHOD

Stretchable Membrane Culture

The device used to stretch cells is described previously.²³ Briefly, human airway smooth muscle (HASM) cells were cultured inside a plexiglass cylindrical well whose bottom surface was a $76\text{-}\mu\text{m}$ thick, uniformly stretched silicon elastomer membrane (Dow Corning, Midland, MI) acting as the cell substrate. The degree of membrane stretch was controlled by pushing a hollow plexiglass cylindrical platen against the membrane. Consequently, the membrane rapidly stretched and distended the cells that adhere to it. Calibration measurements showed that the membrane stretches uniformly, without slipping or relaxing, for membrane strains ranging from 0% to 45%.²³ Membrane strain was defined as a percentage change in the distance between a pair of points on the membrane well relative to their distance before stretching. The stretching device was placed inside the magnetic cytometer in order to measure changes in cell stiffness in response to membrane stretching.

Cell Culture

All measurements were done on cultured HASM cells. Detailed culture procedure was described earlier.¹⁵ Briefly, cells were isolated from tracheal muscle of human lung transplant donors (approved by the University of Pennsylvania Committee on Studies Involving Human Subjects), as described previously.²¹ Cells at passage 6–8 were used; smooth muscle mor-

phology was maintained in HASM cells until at least passage 8.²¹ After cells reached confluence in plastic dishes, they were serum deprived for 48 h before being trypsinized. The membrane well was coated with collagen-I (0.2 mg/ml) and allowed to set overnight. The cells were plated on the membrane (18,000 cells/well), in a serum-deprived medium with 3% BSA added, and allowed to incubate at 37°C for approximately 16 h to reach subconfluence. Care was taken to ensure that cells did not get injured during stretching by plating cells only on the part of the membrane that did not directly contact the platen (see Rosenblatt et al.²³).

Stiffness Measurements

Cell stiffness was measured using the magnetic oscillatory cytometry system as described previously.^{5,7} Small ($4.5\text{-}\mu\text{m}$ diameter) ferromagnetic beads were coated with RGD (Arg–Gly–Asp) peptide that binds specifically to integrin receptors on the cell apical surface. Approximately $10\ \mu\text{g}$ of the RGD-coated beads were added to the plated wells and cells incubated for 10 min. Beads that were not bound to either cells or the membrane were washed away with serum-free medium, and cells were maintained in $300\ \mu\text{l}$ of the serum-deprived medium for the duration of the testing. The beads (3–4 beads per cell on average) were first magnetized by a horizontal magnetic field and then twisted by a sinusoidally varying (0.75 Hz) vertical magnetic field (amplitude $\sim 50\ \text{G}$), for 5 cycles. We chose 5 cycles both to be consistent with previous protocols for bead twisting at 0.75 Hz,⁶ as well as to limit the time course over which non-mechanical effects interfered with our measurements. The horizontal displacement of beads was traced by a charge-coupled device camera (Hamamatsu C4742-95-12ERG) mounted on an inverted microscope (Leica DM IRE2). We analyzed the displacements of approximately 100–120 beads per well that were in the field of view. For each bead, we computed the dynamic stiffness as the complex ratio of the applied specific torque ($\sim 37\ \text{Pa}$) to the corresponding bead displacement (order of $10^2\ \text{nm}$). The ratio was multiplied by a geometrical factor which accounts for the degree of bead internalization and bead-cell geometry²⁰ to obtain the dynamic modulus (G^*) in the units of mechanical stress (in Pa). The real part of G^* is the storage (elastic) modulus (G') and the imaginary part is the loss (viscous) modulus (G''). The ratio of the two, $\eta = G''/G'$, is hysteresivity (loss tangent) indicative of the phase lag between elastic and viscous stresses.¹¹ Beads whose displacement amplitudes were smaller than 20 nm were discarded since the signals were too noisy to accurately determine their displacement. Beads with displacements greater than 650 nm were

discarded in order to insure that the oscillatory response of HASM cells was within the linear range,⁵ a requirement of the Fourier transform technique employed to analyze the data. Discarding beads with large displacements also ensures that we are not tracking beads which are either loosely bound to the cell or which remained attached to the substrate after washing. In addition, beads that yielded values for η that were negative (i.e., the output leads the input presumably due to poor signal-to-noise ratio), as well as beads that clustered together were also discarded. Based on these criteria, about 30–40% of selected beads were not used in final data analysis. This value may be a direct result of choosing a higher lower limit for bead displacements than that established previously (20 vs. 5 nm).⁵ The issue of bead selection is further addressed in Discussion.

Experimental Protocol

Time Controls

Time control measurements were carried out to determine the effects of histamine activation, stretching, and no activation on cell stiffness over time. In all three cases, a single stiffness measurement (0.75 Hz, for 5 cycles) was taken every 45 s in $n = 6$ wells with no activation, in $n = 2$ wells after activation with 10 μ M histamine, and in $n = 2$ wells following 20% membrane stretch.

Stiffness Measurements During Stretching and Retracting

We first determined how external cellular distension affected cell stiffness. For our control group, we measured baseline stiffness prior to stretching ($n = 6$ wells). We then stretched the cells from 0% up to a maximum of \sim 30% membrane strain in step strain increments of \sim 5%. After cells were stretched to \sim 30% strain, the membrane strain was reduced in steps of \sim 5% until the membrane was returned to its baseline of 0% strain. At each stretching and retraction level of substrate strain, we took three measurements of stiffness. For each well, the loading and unloading protocol was done only once. The total time required to complete these measurements at a given stretch was < 1 min.

Stiffness Measurements in Pharmacologically Treated Cells

We next determined how external cellular distension affected stiffness in cells which were either activated or relaxed prior to stretching. We treated $n = 3$ wells with 10 μ M of the contractile agonist histamine and

allowed them to incubate for 30 s, prior to stretching. After incubation, we measured baseline stiffness. We then increased substrate strain from 0% to \sim 30% in step increments of \sim 5%, and measured cell stiffness at each level of strain. The protocol was identical to that used for control cells, except that the stretched substrate was not retracted after reaching \sim 30% substrate strain. Again, at each level of strain we took three measurements of stiffness.

Besides contractile actin filaments, there are also passive stress-bearing filaments of the CSK, including non-contractile actin filaments, intermediate filaments, and microtubules. To investigate their contribution to cell stiffening, we treated $n = 4$ wells with 1 mM of the relaxing agonist dibutryl-cyclic adenosine monophosphate (DBcAMP) and allowed them to incubate for 3 min prior to stretching, allowing the drug to reach over 90% of its effect.⁷ DBcAMP was used to increase the 3',5'-cyclic monophosphate in HASM cells, removing basal tone and decreasing the contractility of the cell to a minimum.¹⁵ After incubating, we measured baseline cell stiffness, and then stretched the treated cells between 0% and \sim 30% substrate strain.

To assess the contribution of cytoskeletal F-actin versus other cytoskeletal filaments to stiffening during stretching, we treated cells from a single well with the F-actin disrupting drug cytochalasin D at a concentration of 1 μ g/ml and allowed the cells to incubate for 30 s prior to stretching. After incubation, we took three measures of baseline stiffness. We then stretched the membrane to approximately 10% and 20% strain and again took three measures of stiffness at each of these strains.

To check whether experimental observations were dependent on the order of treatment, we first stretched cells to \sim 20% membrane strain, measured their stiffness three times ($n = 1$ well) and then added 10 μ M histamine. After incubating the cells for 30 s, we again measured stiffness three times. Results were compared with cells that were first activated than stretched.

Stiffness Measurements in Permeabilized Cells

To investigate the contribution of stretch-induced ion channel activation to the observed cell stiffening response as well as to inhibit focal adhesion remodeling and actin polymerization, cells in $n = 3$ wells were permeabilized with saponin as previously described.^{22,24,31} Briefly, cultured cells were washed once with a CSK stabilization buffer (50 mM KCl, 10 mM imidazole, 1 mM EGTA, 1 mM MgSO₄, 0.5 mM dithiothreitol, 5 μ g/ml leupeptin, 0.1 mM phenylmethylsulfonyl fluoride, and 20 mM PIPES, pH 6.5). Cells were then incubated in the same buffer containing saponin (25 μ g/ml) for 8 min at 37°C and

stiffness measurements were taken at 0%, ~2%, ~10%, and ~20% strain. By permeabilizing the cell membrane, we were able to deplete any calcium (Ca^{2+}) or potassium (K^+) gradients that existed between the cell and the extracellular matrix as well as to allow actin monomers to leach out of the cells.²⁴

Data Analysis

We calculated G' and η for each of the selected beads according to the following method. At a given membrane stretch, we took the median values for G' and G'' for all analyzed beads. We obtained η as the ratio of these median values, $\eta = G''/G'$. At a given stretch, we repeated stiffness measurements three times resulting in as many as three distinct values for G' and η for a given well at a given stretch. The major reason for doing this was to test the reproducibility of our data analysis algorithm. If more than 50% of the beads in a given well did not meet the inclusion criteria mentioned above, then the data from that well were discarded from further data analysis.

Due to technical limitations of the cell-stretching device, it was not possible to maintain the same initial level of tension in the membrane or increment the strain consistently among different wells. Different levels of baseline tension prior to stretching results in cells with different levels of prestress; the prestress is defined as the pre-existing tensile stress borne by the CSK prior to the application of an external loading (in this case magnetic twisting torque). Since cell stiffness (i.e., G') is expected to be proportional to the prestress,^{26,32,33} to compare data between wells, we first needed to account for the different baseline stiffnesses. For this reason we present data for G' as a percentage change from baseline. To obtain changes in G' as a function of substrate strain, we first had to estimate strain for each individual well, at each increment.

To quantify the strain in each well at every step, we acquired a digital image of the membrane, using the same microscope as for magnetic bead tracking, for each well at each treatment, and at each level of strain, including baseline. We used image analysis software (NIH Image J) to measure the distance between 10 and 15 randomly chosen markers and compared these distances to those observed on the same image taken at baseline (for details see Rosenblatt et al.²³). The markers were a combination of either beads on different cells, beads that were on the membrane, or marks that were intrinsic to the membrane itself. Strain was defined as the percentage change in distance between a pair of markers relative to their distance before stretching. We and others showed previously that measuring the strain in this manner does not significantly differ

from the strain that would be calculated by measuring the change in distance between only membrane markers.^{23,29} However, it was necessary to use beads attached to cells as markers since most membrane beads were washed off during cell preparation, and there were few noticeable markers intrinsic to the membrane. For each membrane well, the mean strain calculated from 10 to 15 markers was assumed to represent the substrate strain at a given level of stretching. This strain value was also used for all repeated measures at a given stretch.

To compare G' and η obtained from different wells, we grouped data within certain strain ranges or bins. Bins were chosen such that they spanned strain ranges no greater than 5% and when possible, bins contained data from more than one well. Different binning was chosen for the different treatments. Any effects of the arbitrary choice of binning are considered below in Statistical Analysis. For a given strain range, we calculated an average of all individual membrane strains, an average of all corresponding median values of fractional change in G' , and an average of all corresponding values of η .

Statistical Analysis

Due to the variability of strains among wells, it was not always possible to group the strains in similar bins such that we could statistically compare the differences in the stiffening response for all treatments. Thus, we used an alternative method for comparison as follows. We noted that the fractional change in G' as a function of substrate strain, in both control and histamine-treated cells, initially increased to a peak value after which further increase in G' with stretching was inhibited (see Figs. 2 and 4). Using a least square minimization algorithm, we fitted all of median data for the fractional change in G' as a function of substrate strain (ε) for the cases of controls and histamine-treated cells with the following bilinear function

$$G' = (m_1\varepsilon + b_1) + [(m_2 - m_1)\varepsilon + (b_2 - b_1)]u(\varepsilon - a), \quad (1)$$

where m_1 , m_2 , b_1 , and a are free parameters, $b_2 = a(m_1 - m_2) + b_1$, and $u(\cdot)$ represents the unit step function defined as $u(\varepsilon - a) = 1$ for $\varepsilon \geq a$ and $u(\varepsilon - a) = 0$ for $\varepsilon < a$. Importantly, by fitting all data simultaneously, we avoid any bias that may be caused by the arbitrary grouping the data in strain bins. In the fitting procedure, we constrained m_1 to be positive and m_2 to be negative since in that case the function given by Eq. (1) increases linearly with ascending slope m_1 , peaks at $\varepsilon = a$ and then decreases linearly with descending slope m_2 . The parameters b_1 and b_2 are

intercepts of the ascending and descending branches, respectively. In the case of DBcAMP-treated cells, we fitted data with a simple linear regression, $G' = m_1\varepsilon + b_1$, since those data did not appear to exhibit a peak (see Fig. 4). The variances of the above parameters were also calculated from the least square fits which allowed us to use *t*-tests to compare parameter values among the treatments.

For all tests, differences were considered statistically significant if $p < 0.05$.

RESULTS

Results from time-control measurements showed that in histamine-treated cells and non-treated cells there was no apparent change in G' over a period of at least 5 min (Fig. 1). For cells that were stretched to 20% strain, G' exhibited no change from baseline for the first ~ 90 s. Since all stiffness measurements in our study were done within the first minute following stretching (5 cycles, at 0.75 Hz, repeated three times), data from time-control measurements (Fig. 1) suggest that time-dependent changes in G' during this period were negligible.

Increase in substrate stretching from 0% to 20% leads to an increase in G' that peaked at $\sim 20\%$ strain. Upon further substrate stretching (20–30% strain), G' no longer increased with stretching, but showed an apparent decrease (Fig. 2). However, this apparent decrease in G' was not significant, i.e., the descending slope m_2 of Eq. (1) was not significantly different from zero (see Table 1). Gradual unloading of the substrate from 30% to 0% strain caused a substantial drop in G' between 30% and 20% strain. Further decreases in substrate strain from 20% to 0% lead to virtually no changes in G' . Substrate stretching and retracting did

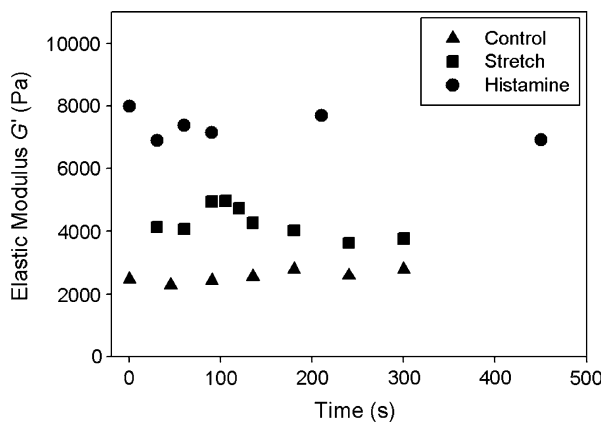


FIGURE 1. The elastic modulus (G') of HASM cells exhibits little dependence on observation time in control, stretched (20%), and histamine-treated (10 μ M) cells. Representative data from one well.

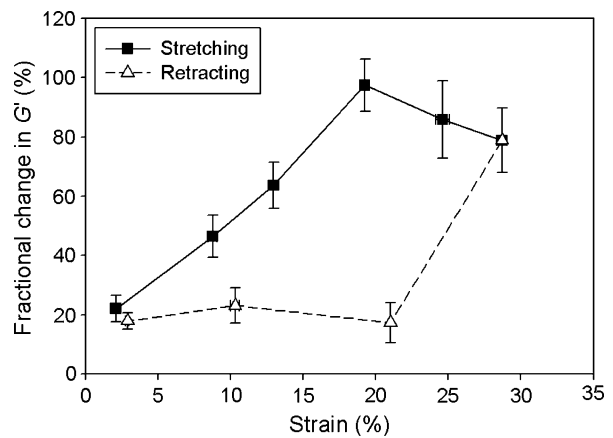


FIGURE 2. Fractional change in the elastic modulus (G') of HASM cells vs. substrate strain during substrate stretching and retracting. The fractional change is calculated relative to the baseline. During stretching, the fractional change in G' increases with increasing substrate strain, peaks and then decreases. During retracting, the fractional change in G' decreases. At a given strain, the fractional change in G' is greater during stretching than during relaxing. Data represent the mean \pm SE of the median values within a given strain range, with the following number of averaged median values: for loading (in order of increasing strain) – 23, 6, 6, 16, 3, 5; for unloading (in order of decreasing strain) – 5, 3, 6, 23. In some cases, the error bars are smaller than the data marker.

not cause systematic changes in η , which remained nearly constant at ~ 0.35 (Fig. 3).

Adding histamine and then stretching did not produce difference in the cell stiffening behavior in comparison with the non-treated (control) cells (Fig. 4). Although the data indicate that histamine-treated cells exhibited smaller fractional changes in G' than control cells, these differences were not significant. Hysteresivity η of histamine-treated cells exhibited little change with substrate strain (Fig. 5) and was not significantly different from controls except at high strains (20–30%) where η of histamine-treated cells was $\sim 25\%$ smaller than that of controls ($p < 0.05$) (Fig. 5). The order of treatments did not affect these findings; similar results were obtained when cells were first stretched and then activated by histamine (data not shown).

In DBcAMP-treated cells, the fractional change in G' monotonically increased with increasing substrate strain (Table 1) but for strains smaller than 10%, it was not significantly different from the baseline value (Fig. 4). Disruption of the actin network by cytochalasin D almost completely abolished stiffening (Fig. 6). Fractional changes in G' measured in permeabilized cells were very similar to those in control cells at $\sim 2\%$ and $\sim 9\%$ substrate strain. However, at higher levels of substrate strain ($\sim 12\%$ and $\sim 20\%$), control cells were significantly stiffer than the saponin-treated cells ($p < 0.05$) (Fig. 7).

TABLE 1. Parameter values obtained by fitting all median data.

	a	m_1	m_2	b_1
Control	20.00 ± 1.53 ($p < 0.0001$)	4.57 ± 0.73 ($p < 0.0001$)	-2.91 ± 1.91 ($p = 0.14$)	9.50 ± 8.64 ($p = 0.276$)
Histamine	19.54 ± 2.69 ($p < 0.0001$)	4.54 ± 0.79 ($p < 0.0001$)	-4.35 ± 3.61 ($p = 0.239$)	-9.39 ± 8.65 ($p = 0.257$)
DBcAMP	–	$1.29 \pm 0.31^*$ ($p = 0.0001$)	–	-3.90 ± 5.50 ($p = 0.481$)

Parameter values are means (SE). The p -values indicate whether the parameters are significantly different from zero ($p < 0.05$); *Significantly different from control and histamine-treated cells.

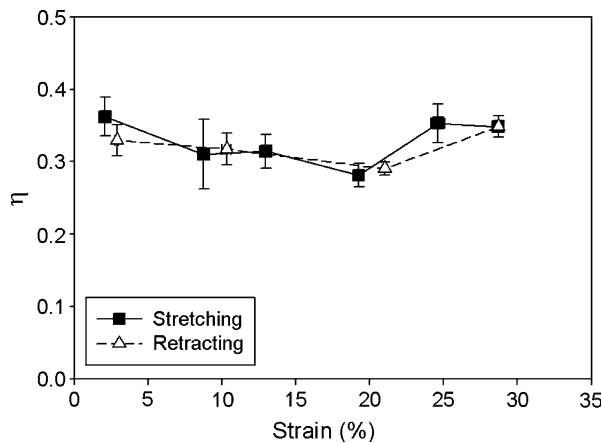


FIGURE 3. Hysteresivity (η) of HASM cells does not change significantly ($p < 0.05$) during both stretching and retracting of the substrate. Data represent the mean \pm SE calculated from the ratio of the median G' value to the median G'' value within a given well, for all wells within a given strain range. The number of median values that were averaged to obtain a point is the same as in Fig. 2.

DISCUSSION

The primary finding of this study is that substrate stretching has a complex influence on cell stiffness and stiffening. First, while at low to mid levels of substrate strains ($< 20\%$) stretching promotes stiffening, at higher strains ($> 20\%$) the increase in stiffening is inhibited (Fig. 2). Second, the hysteresis observed during stretching and retracting of the cells (Fig. 2) indicates irreversibility of the stiffening behavior as well as the contribution of viscoelastic processes. Moreover, our data show that at high levels of substrate strain ($> 20\%$) even a small decrease in substrate strain may lead to a very large decrease in cellular stiffness (Fig. 2). Third, we showed that even when contractile force generation was inhibited by DBcAMP, the CSK could still exhibit stiffening (Fig. 4). Thus, our finding suggests that passive distension of the CSK can provide stiffness to the entire cell and that at high levels of substrate strain this contribution is substantial. Importantly, this passive stiffening response cannot be inferred from experiments on muscle tissue strips since it cannot be discriminated from the stiffening of the extracellular

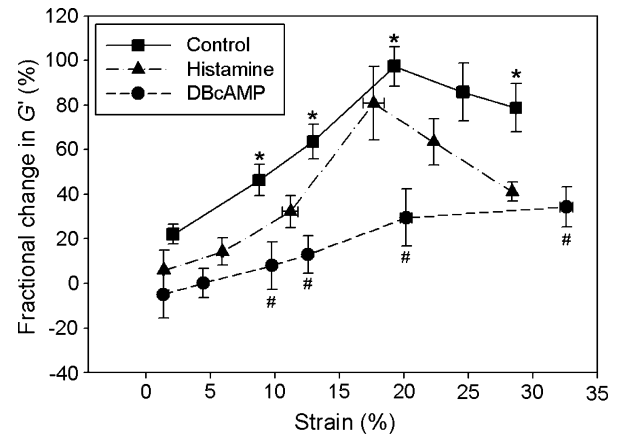


FIGURE 4. Fractional change in the elastic modulus (G') vs. substrate strain during substrate stretching for control, histamine-treated ($10 \mu\text{M}$), and DBcAMP-treated (1 mM) HASM cells. Histamine-treated cells exhibit the same stiffening pattern as control cells (same data as in Fig. 2), whereas the DBcAMP-treated cells exhibit continuous stiffening over the observed substrate strain range. Histamine-treated cells exhibit smaller changes in G' than the control cells but they are not significant. The strain at which the change in G' peaks in histamine-treated cells is lower than, but not significantly different from, the corresponding value in control cells. DBcAMP-treated cells exhibit a significant increase in stiffness from baseline only for substrate strains $> 10\%$ and the values of the fractional change in G' are significantly smaller than those of the control cells. Data represent the mean \pm SE of the median values within a given strain range, with the following number of averaged median values: for histamine-treated cells (in order of increasing strain) – 6, 3, 9, 6, 3, 2 and for DBcAMP-treated cells (in order of increasing strain) – 9, 13, 6, 12, 12, 12. For control cells the numbers are the same as in Fig. 2. In some cases, the error bars are smaller than the data marker; *significant difference between controls and DBcAMP-treated cells; #significantly different from zero for DBcAMP-treated cells ($p < 0.05$).

matrix.¹⁷ Finally, disruption of F-actin by cytochalasin D (Fig. 6) caused a major reduction in cell stiffness and abolishment of stiffening. The last two findings suggest that DBcAMP primarily inhibits the contribution of the contractile machinery to the cell stiffening and not the contribution from the passive distension of the CSK, whereas cytochalasin D inhibits both.

We provide the following interpretation for the above observations with alternative explanations considered later in this section. Mechanical distension of the cell induced by the substrate stretching builds up mechanical

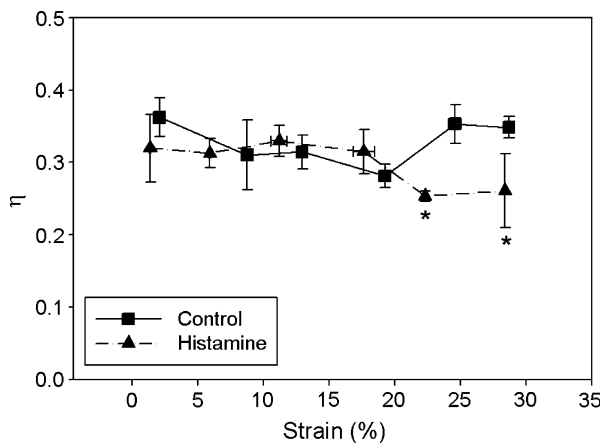


FIGURE 5. Hysteresivity (η) of control and histamine-treated ($10 \mu\text{M}$) HASM cells does not change significantly during loading up to $\sim 20\%$ substrate strain. Above 20% strain, η is significantly lower in histamine-treated than in control cells. Data represent the mean \pm SE of the ratio of the median G'' value to the median G' value within a given well, for all wells within a given strain range. The number of median values that were averaged is the same as in Figs. 2 and 4 for control and histamine-treated cells, respectively. *significantly different from control ($p < 0.05$).

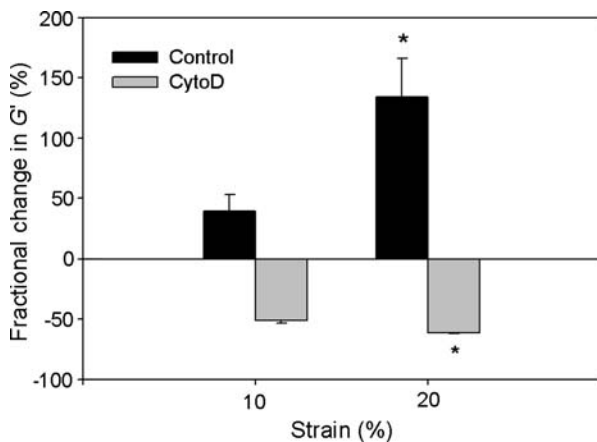


FIGURE 6. Control HASM cells exhibit increased stiffening relative to the baseline level at 10% and 20% substrate strain, whereas cells treated with cytochalasin-D (CytoD, $1 \mu\text{g/ml}$) exhibit softening relative to the baseline level at both 10% and 20% substrate strain. Data for elastic modulus (G') are mean of median values \pm SE from three repeated measurements in a single well. *significantly different from G' at 10% strain.

stress within the CSK that stabilizes the cell through the tensegrity mechanism.²³ Thus, the cell exhibits stiffening behavior. However, excessive cell distension may detach actin myosin cross links causing both the actively generated stress as well as any stress stored during passive distension to dissipate, thereby inhibiting any further buildup of mechanical stress within the cell. Excessive cell distension may also interfere with other non-contractile cytoskeletal filaments, as well as chemical bonds

such as actin–actin or myosin–myosin bonds, or force transmitting pathways that act via actin–integrin receptors. Since these interactions are necessary for the development of cellular force, their destruction would also inhibit the buildup of mechanical stress within the cell. Once the stress dissipation becomes great enough to offset stress buildup at high levels of stretching, the stiffening effect will be inhibited and eventually reversed. This explains our data for non-treated (Fig. 2) and histamine-treated cells (Fig. 4). They suggest that at high levels of distension, a change in the balance between the stress building and stress dissipating processes is occurring.

In DBcAMP-treated cells where baseline tone has been removed, the number of intact actin–myosin cross-bridges prior to stretching is either greatly reduced or, more likely, all cross-bridges are removed and prevented from reforming. In turn, at higher levels of stretching there are far fewer, if any, cross-bridges to detach. Consequently, the inhibition of stress buildup seen in control cells due to the disruption of cross-bridges no longer plays an important roll. Thus, the buildup of the cytoskeletal prestress, predominantly the passive component of the prestress in this case, with increasing substrate stretching is virtually uninterrupted. This would explain the continuous stiffening behavior of DBcAMP-treated cells (Fig. 4), although direct measures of phosphorylation, for example, would help to verify this idea. Still, our findings with DBcAMP-treated cell are novel and indicate the importance of passive distension of the CSK in providing cell shape stability even when cell contractility becomes compromised.

Another possible reason for the observed inhibition of stiffening at high strains for control and histamine-treated cells (Fig. 4), and for the stretching–retracting hysteresis (Fig. 2) could be that cells either partially or completely detached from the substrate during stretching at high strains. We do not believe that this occurred for the following reasons. First, cells did not show signs of rounding up, which would indicate that they had detached from the substrate. Second, if cell detachment from the substrate was responsible for the lack of stiffening at high strains, it should also be observed in the case of the DBcAMP-treated cells, which is not evident in our data (Fig. 4).

Our results showed that the hysteresivity η was not greatly affected by substrate stretching in both control and histamine-treated cells (Figs. 3 and 5) or by stretching and retracting of untreated cells (Fig. 3). Earlier findings in airway smooth muscle tissue suggest that η is proportional to the rate of cross-bridge cycling rather than to the number of cross-bridges attached.⁹ Thus, any difference in the number of cross-bridges attached in control vs. histamine-treated cells and

during stretching vs. retracting should not affect η . Significant differences in η between histamine-treated cells and controls were observed only at very large distensions ($>20\%$ substrate strain) (Fig. 5).

We pointed out that the bead selection process was in part dictated in order to keep the oscillatory measurements within the linear range and in part to ensure that the signal could be distinguished from the noise level. The lower limit used here was 20 nm rather than 5 nm previously reported in the literature.⁵ Although more beads tended to fall within the range of 5–20 nm at higher strains, the noise level for these beads (defined as the mean difference between the data and a sinusoidal fit to the data normalized by the amplitude of the sinusoidal fit) consistently led to their rejection. While approximately 15–30% of all beads fell within the range of 5–20 nm, less than one third of these had an acceptable level of noise. By increasing the number of cycles sampled at a given frequency, we may be able to reduce the number of rejected beads, although this would also increase the impact of any time-dependent effects, such as remodeling, on our measurements. More importantly, when we reduced the lower limit on the bead displacement to 5 nm, and recalculated G' , its median value decreased by approximately 20% across all wells, regardless of strain, when compared to when we chose 20 nm for the lower limit. Since we present data in terms of fractional changes in G' , removing the noisy beads in the range of 5–20 nm should not affect the observed stiffening behavior.

Other factors that could influence cell stiffness and stiffening also include stretch-induced activation of intracellular K^+ and Ca^{2+} ,⁹ cytoskeletal remodeling,^{15,25,33} and focal adhesion remodeling.³ We showed that in saponin-permeabilized HASM cells which lack Ca^{2+} and K^+ gradient, stretch-induced stiffening showed similar trends to those observed in the control state (Fig. 7), suggesting that stretch-induced changes in K^+ and Ca^{2+} have little effect on stiffening below $\sim 10\%$ stretch. These results are consistent with our previous studies performed on permeabilized endothelial cells.²² At higher strains ($\sim 12\%$ and $\sim 20\%$), however, control cells exhibited a substantially greater stiffness than the saponin-treated cells (Fig. 7). We propose the following explanation for these observations. The addition of saponin causes an initial influx of Ca^{2+} , K^+ and ATP, causing many cross-bridges to attach and an initial increase in stiffness. However, disruption of membrane ion channels removes K^+ and Ca^{2+} gradients and prevents cross bridges from cycling, thereby ablating the contribution of active force generation to any observed stiffening during stretch. Upon small stretching ($\sim 2\%$ and $\sim 9\%$), these cells show significant increase in stiffness from baseline (student's t -test, $p < 0.05$) with mean stiffness mea-

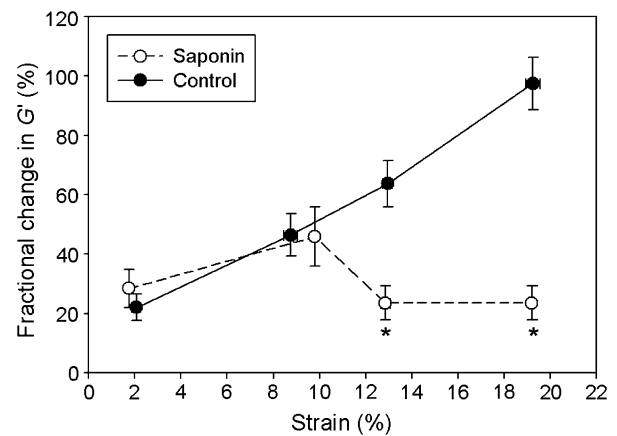


FIGURE 7. At low substrate strains, saponin-treated (permeabilized) HASM cells exhibit similar changes in elastic modulus (G') as control cells. At higher strains, however, saponin-treated cells exhibited a significantly lower change in G' than control cells. Data represent the mean \pm SE of the median values within a given strain range, with the number of median values that were averaged to obtain a point medias follows: for control cells see Fig. 2, for saponin (in order of increasing strain) – 6, 3, 3, 6. Statistical comparison could be performed for the two highest strains between the treatments. *Saponin significantly different from control ($p < 0.05$).

ures nearly identical to those seen in non-permeabilized cells. While the mean fractional change in stiffness increased by nearly 70% from 2% strain to 9% strain this increase was not significant, although we attribute this to the fact that the data sets are very small (2 wells at 2% strain and 1 well at 9% strain). However, at very high substrate strains ($>10\%$), we noted a decrease in stiffness and a change from baseline that is significantly lower than that seen in control cells. We did not observe changes in cell-projected area in permeabilized cells indicating that the cells remained intact at high strains. The decreased stiffening then may be due to the fact that cross bridges detach due to high mechanical distension and may not be able to reattach due to lack of Ca^{2+} and other soluble molecules found in non-permeabilized cells. It is also possible that increasing levels of distension did not provide sufficiently high stress to detach the very stiff cross-bridges formed after cell permeabilization, and thus the decreased stiffness may result from the local rupturing of the non-contractile cytoskeletal elements. Regardless, the observed stiffening at low strains in saponin-treated cells indicates that in the absence of the cross-bridge dynamics, membrane integrity and calcium influx, the cell can still provide stiffening through passive distension as explained by the tensegrity mechanism.

In several studies, agonist-induced cytoskeletal remodeling (defined as any changes in the cytoskeletal structure due to active processes in the cell, including actin polymerization/depolymerization or new

crosslink formation) during contractile stimulation has been implicated as a key mechanism responsible for the observed stiffening of airway smooth muscle cells.^{2,13,19,25,28} Although the two cannot be separated, we believe that our experiments are performed on time scales (within 1 min) that are too short for actin-polymerization and CSK remodeling to occur. This is supported by our time control data (Fig. 1) which indicate that there is little change in stiffness occurring over 1 min. Additionally, *in vitro* studies on actin show that the time constant for actin polymerization is ~ 7 min,³⁰ while studies on stimulated cells required upwards of 15 min before significant polymerization was observed.⁴ In addition, saponin-treated cells show stretch-induced stiffening²⁴ (Fig. 7) even though actin polymerization is inhibited.²⁴ Together, this would suggest that stretch-induced changes in the distending stress in the CSK are the primary cause for altering cell stiffness. However, future studies should consider using direct observations including CSK imaging or measuring the ratio of filamentous to globular actin to verify this.

Aside from depolymerizing the actin-myosin crosslinks, DBcAMP also causes depolymerization of actin.¹⁴ However, the latter effect does not seem to be as prominent as in the case of cells treated with cytochalasin D, since in cytochalasin D-treated cells, depolymerization abolishes the stiffening (Fig. 6) whereas in DBcAMP-treated cells stiffening is prominent (Fig. 4). Hirshman et al.¹⁴ showed that adding 100 μ M of cAMP-dependent protein kinase A agonist (Sp-cAMPS) to HASM cells over 30 min causes reduction in the ratio of filamentous to globular actin by only $\sim 20\%$, whereas our measurements took place ~ 3 min after DBcAMP treatment, although at the higher concentration (1 mM). On the other hand, these authors also showed that adding vasodilators isoproterenol and forskolin to HASM cells, both of which increase cytosolic cAMP, decreases the filamentous to globular actin ratio by more than 50% within 5 min of the treatment.¹⁴ Taken together, these results suggest that it is likely that both actin depolymerization and reduced actin-myosin activity led to the DBcAMP-reduced stretch-induced stiffening of Fig. 4.

Modulation of contractile stress may also affect focal adhesion formations³ that were shown to occur within the time period of our experiments. While we cannot rule out the effect of focal adhesion remodeling, our results with saponin treatment, which should greatly decrease the extent of focal adhesion remodeling, suggests that it has little contribution to cell stiffening during stretching, at least up to $\sim 10\%$ substrate strain. At the same time, it may be that the inhibition of focal adhesion remodeling in saponin-

treated cells is the cause for the structural instability observed at high strains, since, under physiologic conditions, applied stretch initiates focal adhesion growth which in turn enables the cell to maintain higher levels of distending stress.¹² However, much of this work focuses on initial focal adhesion complex changes in response to initial integrin activation after bead binding and after quick force application. This behavior is mostly at the receptor-ligand-focal adhesion vicinity. Our cell stiffness measurements reflect the contribution from the deep CSK.¹⁸ Thus, the previously observed relationships between focal adhesion growth and force application may not be relevant here.

Finally, since a portion of G' as measured by bead twisting cytometry is influenced by the cell thickness, it is possible that the observed stiffening does not result mainly from the storage of passive distending, but rather from decrease in cell thickness during stretching.^{8,20} We do not believe, however, that this stretch-induced cell thinning plays a major role in the stiffening response observed. This effect becomes important when cell thickness is less than 1 μ m, and even then it can produce only a moderate stiffening (0–20%) which is smaller than the observed changes.^{20,22}

Our findings also help to reconcile two distinct mechanisms that have previously been used to explain stiffening of airway smooth muscle cells – tensegrity^{26,32,33} and myosin cross-bridge recruitment.^{9,10} The tensegrity model predicts that cell stiffness depends on prestress in the CSK, whereas myosin cross-bridge recruitment predicts that cell stiffness depends on the number of attached cross bridges. However, predictions from the tensegrity model are independent of whether the prestress is generated actively, by cross bridge kinetics, or passively, by substrate distension. In this sense, then the two mechanisms are not truly distinct. Our results show that these mechanisms work together to contribute to cell stiffness. Future studies could include the effects of cyclic substrate stretching and the effects of stretching frequency in cell stiffening to mimic more physiologic conditions.

In summary, the results of this study suggest that distending stress of both the active stress generation of the CSK and passive distension of the CSK contribute to the stiffening behavior of living HASM cells under physiological conditions, but that at high levels of distensions there is a possible tradeoff between these two components with the contribution from the passive distension of the CSK becoming increasingly more important. These findings may have implications for the understanding of how the contractile state of airway smooth muscle cells together with stretching of both the cellular and connective tissue components of the airways during breathing might play a role in setting the caliber of the airway lumen.

ACKNOWLEDGMENT

This work was supported by NIH Grants HL-33009 and GM-072744.

REFERENCES

- ¹An, S. S., R. E. Laudadio, J. Lai, R. A. Rogers, and J. J. Fredberg. Stiffness changes in cultured airway smooth muscle cells. *Am. J. Physiol. Cell Physiol.* 283:C792–C801, 2002.
- ²Bursac, P., G. Lenormad, B. Fabry, M. Oliver, D. A. Weitz, V. Viasnoff, J. P. Butler, and J. J. Fredberg. Mechanism unifying cytoskeletal remodeling and slow dynamics in living cells. *Nat. Mater.* 4:567–561, 2005.
- ³Chen, C. S., J. L. Alonso, E. Ostuni, G. M. Whitesides, and D. E. Ingber. Cell shape provides global control of focal adhesion assembly. *Biochem. Biophys. Res. Commun.* 307:355–361, 2003.
- ⁴Deng, L., N. J. Fairbank, B. Fabry, P. G. Smith, and G.N. Maksym. Localized mechanical stress induces time-dependent actin cytoskeletal remodeling and stiffening in cultured airway smooth muscle cells. *Am. J. Physiol. Cell Physiol.* 287:C440–C448, 2004.
- ⁵Fabry, B., G. N. Maksym, J. P. Butler, M. Glogauer, D. Navajas, and J. J. Fredberg. Scaling the microrheology of living cells. *Phys. Rev. Lett.* 87:148102.
- ⁶Fabry, B., G. N. Maksym, J. P. Butler, M. Glogauer, D. Navajas, N. A. Taback, E. J. Millet, and J. J. Fredberg. Time scale and other invariants of integrative mechanical behavior in living cells. *Phys. Rev. E* 68:041914–04191418, 2003.
- ⁷Fabry, B., G. N. Maksym, S. A. Shore, P. E. Moore Jr., R. A. Panettieri, J. P. Butler, and J. J. Fredberg. Signal transduction in smooth muscle selected contribution: Time course and heterogeneity of contractile responses in cultured human airway smooth muscle cells. *J. Appl. Physiol.* 91:986–994, 2001.
- ⁸Féréol, S., R. Fodil, B. Labat, S. Galiacy, V. M. Laurent, B. Louis, and D. Isabey. Sensitivity of alveolar macrophage to substrate mechanical and adhesive properties. *Cell Motil. Cytoskeleton* 63:321–340, 2006.
- ⁹Fredberg, J. J., D. Inouye, B. Miller, M. Nathan, S. Jafari, S. H. Raboudi, J. P. Butler, and S. A. Shore. Airway smooth muscle, tidal stretch, and dynamically determined contractile stress. *Am. J. Respir. Crit. Care Med.* 156:1752–1759, 1997.
- ¹⁰Fredberg, J. J., K. A. Jones, M. Nathan, S. Raboudi, Y. S. Prakash, S. A. Shore, J. P. Butler, and G. C. Sieck. Friction in airway smooth muscle: mechanism, latch, and implications in asthma. *J. Appl. Physiol.* 81:2703–2712, 1996.
- ¹¹Fredberg, J. J. and D. Stamenović. On the imperfect elasticity of lung tissue. *J. Appl. Physiol.* 67:2408–2419, 1989.
- ¹²Galbraith, C. G., K. M. Yamada, and M. P. Sheetz. The relationship between force and focal complex development. *J. Cell Biol.* 159:695–705, 2002.
- ¹³Hirshman, C. A. and C. W. Emala. Actin organization in airway smooth muscle cells involves Gq and Gi-2 activation of Rho. *Am. J. Physiol. Lung Cell Mol. Physiol.* 277:L653–L661, 1999.
- ¹⁴Hirshman, C. A., D. Zhu, R. A. Panettieri, and C. W. Emala. Actin depolymerization via β -adrenoceptor in airway smooth muscle cells: a novel PKA-independent pathway. *Am. J. Physiol. Cell Physiol.* 281:C1468–C1476, 2001.
- ¹⁵Hubmayr, R. D., S. A. Shore, J. J. Fredberg, E. Planus, R. A. Panettieri Jr., W. Moller, J. Heyder, and N. Wang. Pharmacological activation changes stiffness of cultured human airway smooth muscle cells. *Am. J. Physiol. Cell Physiol.* 271:C1660–C1668, 1996.
- ¹⁶Ingber, D. E.. Cellular tensegrity revisited I. Cell structure and hierarchical systems biology. *J. Cell. Sci.* 116:1157–1173, 2003.
- ¹⁷Ito, S., A. Majumdar, H. Kume, K. Shimokata, K. Naruse, K. R. Lutchen, D. Stamenović, and B. Suki. Viscoelastic and dynamic nonlinear properties of airway smooth muscle tissue: roles of mechanical force and the cytoskeleton. *Am. J. Physiol. Lung Cell Mol. Physiol.* 290:L1227–L1237, 2006.
- ¹⁸Laurent, V. M., R. Fodil, P. Cañadas, S. Féréol, B. Louis, E. Planus, and D. Isabey. Partitioning of cortical and deep cytoskeleton responses from transient magnetic bead twisting. *Ann. Biomed. Eng.* 31:1263–1278, 2003.
- ¹⁹Mehta, D. and S. J. Gunst. Actin polymerization stimulated by contractile activation regulates force development in canine tracheal smooth muscle. *J. Physiol. (Lond.)* 519:829–840, 1999.
- ²⁰Mijailovich, S. M., M. Kojic, M. Zivkovic, B. Fabry, and J. J. Fredberg. A finite element model of cell deformation during magnetic bead twisting. *J. Appl. Physiol.* 93:1429–1436, 2002.
- ²¹Panettieri, R. A., R. K. Murray, L. R. DePalo, R. A. Yadvish, and M. I. Kotlikoff. A human airway smooth muscle cell line that retains physiological responsiveness. *Am. J. Physiol. Cell Physiol.* 256:C329–C335, 1989.
- ²²Pourati, J., A. Maniotis, D. Spiegel, J. L. Schaffer, J. P. Butler, J. J. Fredberg, D. E. Ingber, D. Stamenović, and N. Wang. Is cytoskeletal tension a major determinant of cell deformability in adherent endothelial cells? *Am. J. Physiol. Cell Physiol.* 274:C1283–C1289, 1998.
- ²³Rosenblatt, N., S. Hu, J. Chen, N. Wang, and D. Stamenović. Distending stress of the cytoskeleton is a key determinant of cell rheological behavior. *Biochem. Biophys. Res. Commun.* 321:617–622, 2004.
- ²⁴Sims, J. R., D. Karp, and D. E. Ingber. Altering the cellular mechanical force balance results in integrated changes in cell, cytoskeletal and nuclear shape. *J. Cell Sci.* 103:1215–1222, 1992.
- ²⁵Smith, B. A., B. Tolloczko, J. G. Martin, and P. Grütter. Probing the viscoelastic behaviour of cultured airway smooth muscle cells with atomic force microscopy: stiffening induced by contractile agonist. *Biophys. J.* 88:2994–3007, 2005.
- ²⁶Stamenović, D. Effects of cytoskeletal prestress on cell rheological behavior. *Acta Biomater.* 1:255–262, 2005.
- ²⁷Stamenović, D., and N. Wang. Invited review: engineering approaches to cytoskeletal mechanics. *J. Appl. Physiol.* 89:2085–2090, 2000.
- ²⁸Tang, D., D. Mehta, and S. J. Gunst. Mechanosensitive tyrosine phosphorylation of paxillin and focal adhesion kinase in tracheal smooth muscle. *Am. J. Physiol. Cell Physiol.* 276:C250–C258, 1999.
- ²⁹Trepap, X., M. Grabulosa, F. Puig, G. N. Maksym, D. Navajas, and R. Farré. Viscoelasticity of human alveolar epithelial cells subjected to stretch. *Am. J. Physiol. Lung Cell Mol. Physiol.* 287:L1025–L1034, 2004.
- ³⁰Wachssotck, D. H., W. H. Schwartz, and T. D. Pollard. Cross-linker dynamics determine the mechanical properties of actin gels. *Biophys. J.* 66:801–809, 1994.

- ³¹Wang, N. and D. E. Ingber. Control of the cytoskeletal mechanics by extracellular matrix, cell shape, and mechanical tension. *Biophys. J.* 66:2181–2189, 1994.
- ³²Wang, N., K. Naruse, D. Stamenović, J. J. Fredberg, S. M. Mijailovich, I. M. Tolić-Nørrelykke, T. Polte, R. Mannix, and D. E. Ingber. Mechanical behavior in living cells consistent with the tensegrity model. *Proc. Natl. Acad. Sci. USA* 98:7765–7770, 2001.
- ³³Wang, N., I. M. Tolić-Nørrelykke, J. Chen, S. M. Mijailovich, J. P. Butler, J. J. Fredberg, and D. Stamenović. Cell prestress, stiffness I., and prestress are closely associated in adherent contractile cells. *Am. J. Physiol. Cell Physiol.* 282:C606–C616, 2002.